




Cite this: *Soft Matter*, 2023,  
19, 282

Received 3rd September 2022,  
Accepted 7th December 2022

DOI: 10.1039/d2sm01193j

[rsc.li/soft-matter-journal](https://rsc.li/soft-matter-journal)

# Polymer sequence design *via* molecular simulation-based active learning†

Praneeth S Ramesh and Tarak K Patra \*

Molecular-scale interactions and chemical structures offer an enormous opportunity to tune material properties. However, designing materials from their molecular scale is a grand challenge owing to the practical limitations in exploring astronomically large design spaces using traditional experimental or computational methods. Advancements in data science and machine learning have produced a host of tools and techniques that can address this problem and facilitate the efficient exploration of large search spaces. In this work, a blended approach integrating physics-based methods, machine learning techniques and uncertainty quantification is implemented to effectively screen a macromolecular sequence space and design target structures. Here, we survey and assess the efficacy of data-driven methods within the framework of active learning for a challenging design problem, *viz.*, sequence optimization of a copolymer. We report the impact of surrogate models, kernels, and initial conditions on the convergence of the active learning method for the sequence design problem. This work establishes optimal strategies and hyperparameters for efficient inverse design of polymer sequences *via* active learning.

## 1. Introduction

Copolymers are a class of macromolecules that are prepared by combining two or more different types of chemical moieties using appropriate polymerization and synthesis techniques.<sup>1–5</sup> Optimal properties of copolymers intended for specific applications, such as interfacial energy, selective chemical transport behaviour (proton, ion, or water transport), structural phase transitions, the kinetics of biodegradation, and drug release profiles, have been found to be strongly dependent on the precise sequence of copolymer chains.<sup>6–13</sup> A wide range of phases and aggregates are achieved by controlling the sequence of a copolymer.<sup>14–16</sup> In many cases, this sequence-specificity is so profound that a subtle change in the copolymer sequence results in a significant change in the properties of interest.<sup>17–19</sup> Often times, the optimal property is present in a non-intuitive, seemingly arbitrary polymer sequence, the sequence-specificity of which cannot be approximated by coarse sequence statistics or mean-field theories.<sup>20–22</sup> The observation that sequence-specificity is crucial for property optimization is well known in biological systems, wherein sequence-specific macromolecules such as proteins, lipid bilayers, ribonucleic acids, and

deoxyribonucleic acids have been optimized by nature for their functionalities over millions of years of natural evolution.<sup>23</sup> Although the sequence control offers great scope for tuning properties, a systemic approach for identifying optimal sequences for a design problem is an enormous task. Intuition-based material design approaches/rudimentary trial-and-error approaches would fetch limited results,<sup>7</sup> while on the other hand, brute-force approaches enumerating the entire range of sequence possibilities and measuring/computing their properties are time-consuming, laborious, inefficient, and impractical. Even for a simple linear AB-type copolymer of chain length 100, the brute-force enumeration would result in 2<sup>99</sup> sequences which are over 10<sup>29</sup> possibilities. The sequence possibilities would be exceedingly higher for longer copolymer systems comprising several monomer constituents. A feasible and viable approach is therefore necessary for intelligently identifying sequences that are more likely to have a particular desired property, and the available resources, time, and effort could be channelized towards a smaller set of sequence configurations rather than exhaustively scanning the entire sequence space. Such an efficient exploration of vast search spaces can be done with the help of certain tools and techniques that have emerged recently in the wake of the latest advancements in data science and artificial intelligence.<sup>24–26</sup> Therefore, a blended approach that integrates physics-based methods and data science techniques offers efficient ways of screening a copolymer's sequence space. Moreover, developing such strategies that are fast, efficient, and scalable for exploring the sequence space of a macromolecule is demanding

Department of Chemical Engineering, Center for Atomistic Modeling and Materials Design and Center for Carbon Capture Utilization and Storage, Indian Institute of Technology Madras, Chennai, TN 600036, India. E-mail: [tpatra@iitm.ac.in](mailto:tpatra@iitm.ac.in)

† Electronic supplementary information (ESI) available. See DOI: <https://doi.org/10.1039/d2sm01193j>

as sequence engineering is becoming a promising route for materials design.

Advanced optimization methods and machine learning tools such as evolutionary computing, Monte Carlo tree search, and generative models have been progressively combined with physics-based methods such as molecular dynamics (MD) simulations for tackling inverse design problems.<sup>7,17,27</sup> Along this line, active learning (AL) has emerged as a faster and more efficient tool for screening materials' conformational space.<sup>28–31</sup> AL algorithms actively search for new candidates in the design space and progressively rebuild a predictive model with increasing amounts of training data. In an AL cycle, newer data points are strategically selected based on the principles of Bayesian inferences.<sup>32</sup> The first step of the active learning framework involves estimating the objective function through a surrogate model implemented over a training set. The premise is to obtain a proxy for the objective function through a computationally cheap pathway. Machine-Learning (ML) models such as Gaussian process regression, support vector regression, and kernel ridge regression are frequently used for this purpose.<sup>33</sup> These surrogate models are then used to make computationally cheap predictions of properties for a set of candidate structures in the search space. The surrogate predictive model also provides uncertainty measures for every prediction.<sup>34</sup> The uncertainty, in some sense, is a quantitative description of the degree to which a new candidate falls within/outside the domain of the training dataset. The estimates of the prediction values and the uncertainty values are crucial in selecting the candidate copolymer sequences for which computation of properties would be the most strategic. This is the second step of active learning, in which a few candidates are selected for property computation through physics-based methods. These new data are then appended to the training set, and the surrogate model is rebuilt using a slightly larger training set. These two steps are repeated iteratively, and a progressively expanding training set is generated so as to continuously update and refine the surrogate model. Usually, ML models make better predictions when their training data set is large. Therefore, it is expected that an AL algorithm will converge faster toward an optimal solution as the training data set grows over iterations. However, the performance of an AL algorithm appears to be sensitive to the choice of its surrogate model and associated kernel, selection of hyperparameters in the surrogate model, and the query strategy. These factors have been studied recently, and efficient AL pathways are explored for several materials design problems,<sup>32,33,35–37</sup> but their adaptation and implementation for macromolecular design problems are quite rare. Here, we aim to examine and establish the most efficient active learning pathway for screening a macromolecular conformational space and its design for a target property. We note that machine learning models are established to predict sequence-defined properties of polymers.<sup>26,38–40</sup> These models are very powerful and can be used for high-throughput screening and the design of polymers. However, these models are built on a larger amount of pre-existing sequence-property data that are calculated using molecular simulations *a priori*.

In contrast, here, we aim to generate sequence-property data on-the-fly during a design cycle. We expect that such an active learning method will produce a minimal amount of sequence-property data, which are computationally expensive, for a given design problem. Therefore, the data generation is targeted toward optimal candidates. Since the evolution of the design algorithm is based on physics-based property calculations and not on the basis of an ML model predicted properties, it guarantees that the designed molecule will have the target properties. Such an active learning method for a sequence problem is recently explored by Jablonka *et al.*<sup>41</sup>

Here the objective is to establish an efficient active learning strategy within the Bayesian optimization framework to select a minimal number of candidate sequences intelligently for expensive physics-based computations, and thus accelerate copolymer design. As a representative case, we consider the sequence design of an AB-type copolymer for a target structure. We aim to identify the sequence of an AB-type copolymer that possesses a target radius of gyration in an implicit solvent. The radius of gyration is an important design parameter for polymeric materials as it is correlated to a polymer's bulk density, thermal conductivity, viscosity and many other properties.<sup>41–43</sup> Moreover, computing the radius of gyration of a polymer is computationally cheap. Therefore, we choose the radius of gyration as a target property for testing and validating the design framework. We conduct coarse-grained molecular dynamics simulations of the copolymer in an implicit solvent environment for estimating the radius of gyration of candidate sequences during an active learning cycle. Fingerprinting of the 100-mer AB-type copolymer sequence is done by coding the As by 1s and Bs by 0s, and this defines the input variables. We first analyze different nuances of the Bayesian Optimization approach, such as the choice of the surrogate model and associated kernel, selection of hyper-parameters in surrogate models, number of iterations required for convergence, stopping criterion, rate of progress towards convergence, and model quality across iterations, for a case study whose final solution is known analytically. Subsequently, an AB-type copolymer system of chain length 100 with the number of As and Bs constrained to be in a 50 : 50 ratio is considered, and the best active learning framework is implemented to find the optimal sequence with the lowest radius of gyration value. The AL algorithm efficiently identifies the optimal sequence for the lowest radius of gyration that appears to be a protein-like core-shell structure. The capability of the active learning framework to identify such non-intuitive optimal sequences with complex structures is successfully demonstrated.

## 2. Model and methodology

### 2.1. Model polymer

We consider the Kremer–Grest bead-spring model<sup>41–44</sup> of a copolymer to explore its sequence space *via* active learning. In this model system, two adjacent coarse-grained monomers of a polymer are connected by the Finitely Extensible Nonlinear Elastic

(FENE) potential of the form  $E(r) = -\frac{1}{2}KR_0^2 \ln \left[ 1 - \left( \frac{r}{R_0} \right)^2 \right]$ , where  $K = 30 \text{ } \varepsilon/\sigma^2$  and  $R_0 = 1.5\sigma$  for  $r \leq R_0$ , and  $E(r) = \infty$  for  $r > R_0$ . The pair interaction between any two monomers is modeled by the Lennard-Jones (LJ) potential of the form  $V(r) = 4\varepsilon \left[ \left( \frac{\sigma}{r} \right)^{12} - \left( \frac{\sigma}{r} \right)^6 \right]$ .  $\varepsilon$  is the unit of pair interaction energy, and the size of all the monomers is  $\sigma$ . The LJ interaction is truncated and shifted to zero at a cut-off distance  $r_c = 2.5\sigma$  to represent attractive interaction between the monomers. The AA interaction strength is  $\varepsilon_{AA} = \varepsilon$ , while the BB and AB interaction strengths are  $\varepsilon_{BB} = \varepsilon_{AB} = 0.2\varepsilon$ . This ensures immiscibility between A and B-type monomers and is used to understand the generic phase behaviour of copolymers.<sup>45,46</sup> We choose copolymers of chain length  $N = 20$  to  $N = 150$  in this study.

## 2.2. Molecular dynamics simulations

We conduct implicit solvent molecular dynamics simulations of a polymer chain in a canonical ensemble. The initial configuration of a polymer chain is placed in a cubic simulation box of fixed dimensions, and the box is periodic in all three directions. The size of the simulation box is  $45\sigma$ . We use the velocity Verlet algorithm with a time step of  $0.001\tau$  to integrate the equation of motion. Here,  $\tau = \sigma\sqrt{m/\varepsilon}$  is the unit of time, and  $m$  is the mass of a monomer, which is the same for both A and B type moieties. All the simulations are conducted at a reduced temperature  $T^* = Tk_B/\varepsilon = 1$ , which is maintained by the Langevin thermostat within the LAMMPS simulation environment.<sup>47,48</sup> Here,  $k_B$  is the Boltzmann constant and  $T$  is the actual temperature. All the simulations are equilibrated for  $10^8$  MD steps followed by a production run of  $10^8$  MD steps. The data during the production cycles are collected for computing the radius of gyration of a polymer chain.

## 2.3. MD-based active learning

The Bayes' theorem describes the posterior distribution  $P(f|D)$  of an event based on its prior probability and likelihood function, which can be written as  $P(f|D) = \frac{P(D|f)P(f)}{P(D)}$ , where  $P(f)$  is the prior probability distribution and  $P(D|f)$  is the likelihood function. The denominator  $P(D)$  is the marginal likelihood or evidence, which is usually computationally intractable, and is merely a normalizing constant. Here,  $D$  is the given data set. In essence,  $P(f|D) \propto P(D|f)P(f)$ . The prior  $P(f)$  represents *a priori* belief about the space of possible objective functions before any data are taken into consideration. Although the precise functional detail of the function  $f$  remains unknown without any data, prior knowledge about some of the properties of the objective function such as the assumption of its smoothness is captured by the prior function. As we accumulate data  $D\{X, Y\}$ , where  $X$  refers to the set of copolymer sequences and  $Y$  refers to the corresponding radius of gyration, the prior distribution is combined with the likelihood function  $P(D|f)$  to obtain the posterior which captures our updated beliefs about the unknown objective function, *i.e.*, the radius of gyration.<sup>49</sup>

Materials design framework can be established based on this Bayesian approach of relating posterior distribution and prior probability. As shown in Fig. 1, a training set  $X_{\text{train}}$  is defined by randomly selecting 112 copolymer sequences from the vast combinatorial space of  $2^{99}$  sequences. We begin with an A-type homopolymer of desired chain length and randomly select a fixed number of monomers. The selected A-type monomers are converted to B-type. The process is continued until we collect 112 distinct sequences. For each of the copolymer sequences that is part of  $X_{\text{train}}$ , the corresponding radius of gyration value is determined through MD simulations so as to populate the corresponding  $Y_{\text{train}}$ . By building a surrogate model over the initial training set of  $\{X_{\text{train}}, Y_{\text{train}}\}$ , computationally

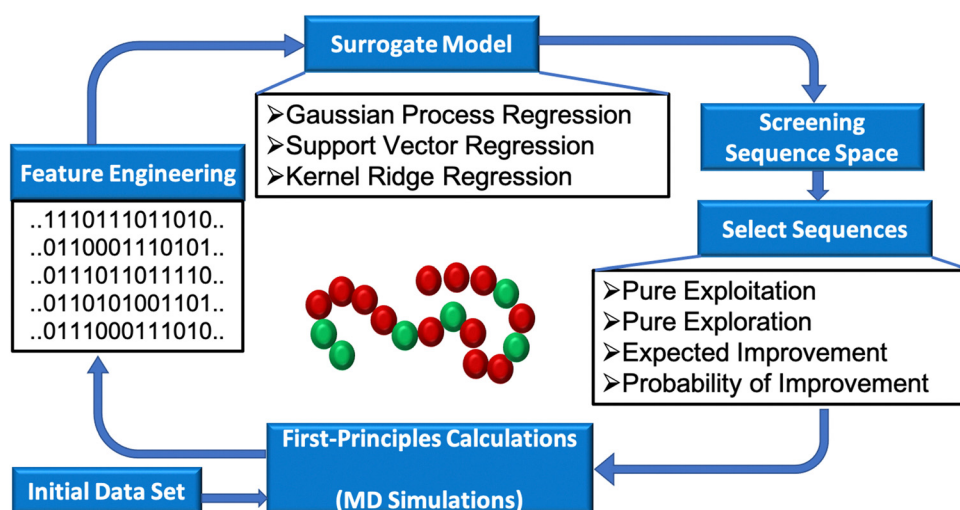


**Fig. 1** Active learning workflow. The initial set of sequences are randomly generated and their properties are calculated using MD simulations. The chemical moieties in these sequences are mapped to a string of 1s and 0s for facilitating easier feature representation. Surrogate models are built based on these data. Subsequently, the sequence space is screened to select a predefined number of candidate sequences, based on the predictions of the surrogate models. MD simulations are then conducted for this set of selected candidates. The process continues until a termination criterion is reached.

cheap predictions of radius of gyration can be obtained for other copolymer sequences whose radius of gyration values are unknown. The estimation of the prediction values by a surrogate model and the quantification of the degree of uncertainty associated with each prediction are crucial elements of the active learning framework. We have used Gaussian process regression (GPR), support vector machine (SVM) and kernel ridge regression (KRR) as surrogate models in this work. GPR directly provides an estimation of the uncertainty of a prediction.<sup>50</sup> However, the SVM and KRR do not estimate uncertainties, and thus a bootstrap approach<sup>51</sup> is employed for obtaining their uncertainties. For each of these three surrogate models, we choose two kernels. Therefore, a total of six surrogate models are considered in this study. The mathematical details of the three surrogate models and their kernels are presented in the ESI,<sup>†</sup> along with five different query strategies. The choice of hyperparameters plays a vital role in governing the quality of these surrogate models and, in turn, the performance of the optimizer.<sup>52,53</sup> Based on our initial studies, we choose a set of hyperparameters for all the surrogate models, which remains fixed during the active learning process. We report the set of hyperparameters for all the models in the ESI.<sup>†</sup>

Now, once the hyperparameters of a surrogate model are chosen and subsequently when the surrogate model has been trained over a training set, it is computationally intractable to run this surrogate model to make predictions over the entire space of copolymer sequences whose radius of gyration values are unknown. Instead, a candidate search space is defined by considering the copolymer sequences that are sequentially proximate to the training set. Predictions and their uncertainties are obtained for all the sequences. A subset of these candidates is shortlisted for first principles-based property estimation. Here we choose 32 candidates for computing their radius of gyration *via* MD simulations. This selection is done according to different query strategies namely pure exploitation, pure exploration, and using acquisition functions such as maximum expected improvement (Max-EI) and maximum probability of improvement (Max-PI). A random selection of sequences is also performed to serve as a baseline to which the performance of the different query strategies could be compared with. With six models, and five query strategies

(including the random selection), a total of 30 optimization frameworks are tested here for the sequence design problem. Therefore, the active learning process comprises of several sequential steps, *viz.*, training the surrogate model using the available data, defining a candidate search space, running the model to estimate predictions and uncertainties, selecting candidates based on a query strategy, and computing the radius of gyration of the selected candidates by MD simulations. These sequential steps are repeated in an iterative manner until convergence criteria are met, as shown in Fig. 1. An open-sourced application programming interface, *viz.*, scikit-learn,<sup>54,55</sup> is integrated with LAMMPS to build the AL models. The scikit-learn library functions, which are used in the AL frameworks, are discussed in ESI.<sup>†</sup>

### 3. Results and discussion

We begin with validating the model and the method that are used for calculating the radius of gyration ( $R_g$ ) of single-chain copolymers in an implicit solvent condition. Fig. 2a shows the pair energy and  $R_g$  of a randomly selected copolymer during the production run, which is conducted after its equilibration. The MD snapshots of the initial and final configuration are shown in Fig. 2b and c, respectively. The energy per particle and the  $R_g$  value reach a steady state within our simulation time as demonstrated in Fig. 2a. For this particular polymer chain, the in-equilibrium radius of gyration is  $3.55 \pm 0.10\sigma$ . The statistical fluctuation in  $R_g$  is  $\sim 3\%$ . This is the typical range of error bars in all our data.

#### 3.1. Performance of active learning strategies

To establish, validate and benchmark an efficient active learning framework for the sequence design problem, we first consider a case where the optimal solution can be estimated analytically. Since the cohesive energy of an A-type monomer is higher than that of a B-type monomer in the current model, the copolymer with the lowest  $R_g$  would consist of all A-type monomers for an unconstrained composition ratio. Here, the composition ratio is defined as the ratio of the number of A-type moieties and the number of B-type moieties in a polymer chain. We calculate the

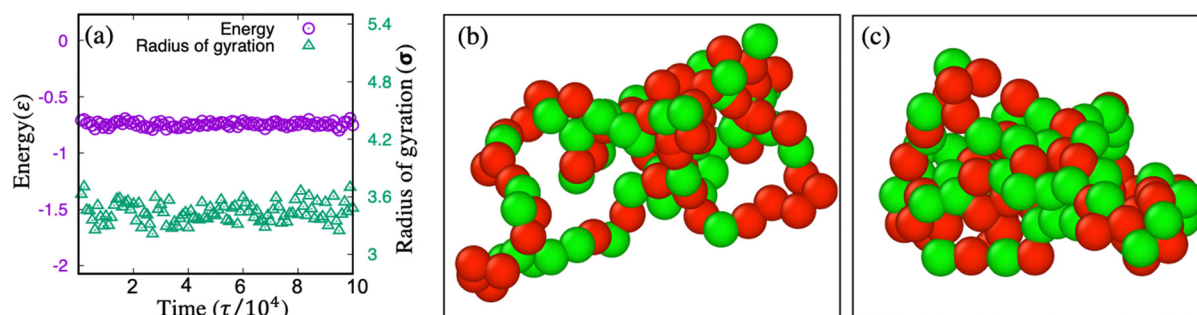


Fig. 2 Validation of the model and method for property calculation. (a) The radius of gyration and pair energy of the system during the production run. (b) The initial configuration of the polymer. (c) The final configuration of the polymer. The red and green beads are type-A and type-B monomers, respectively.



$R_g$  of a polymer of chain length  $N = 100$  that consists of only A-type moieties as  $2.47 \pm 0.08\sigma$ . Therefore, based on the physical understanding of the model system, the lowest average  $R_g$  of a copolymer of chain length  $N = 100$  is  $2.47\sigma$ . Therefore, we consider  $R_g = 2.47\sigma$  for  $N = 100$  as the global optimal value in this design problem and aim to identify candidate polymers with  $R_g = 2.47\sigma$  within the active learning framework, starting from a random sequence of As and Bs. Towards this end, we carry out several active learning studies within the Bayesian optimization (BO) framework for over 75 iterations using six different predictive models (three surrogates with two kernels each) and five query strategies in each model. In each iteration, a total of 32 candidates'  $R_g$  values are directly measured using MD simulations. The initial data set is the same for all the case studies. Being a minimization problem, the performance of the optimizer is primarily assessed by monitoring the way sequences with lower  $R_g$  are identified with increasing MD computations. Fig. 3 shows cumulative plots that represent the minimum  $R_g$  observed so far during an active learning cycle *versus* the number of MD computations performed so far, for all the case studies. Interestingly, three query strategies – pure exploitation, Max-EI and Max-PI – in all cases (a to f), exhibit similar behaviour in approaching towards an average  $R_g$  value of  $2.47\sigma$ . Evidently, pure exploration and random queries in all the cases produce suboptimal solutions where the search is trapped in local minima far away from  $R_g = 2.47\sigma$  for a significant amount of time. From Fig. 3, we infer that the BO with the three query strategies – pure exploitation, Max-EI and Max-PI – iteratively identifies better candidates with a focus on minimizing the objective function, *viz.*,  $R_g$ . The extent of decrease in  $R_g$  over

**Table 1** Number of MD simulations to identify a sequence with an MD run-time average  $R_g$  of  $2.47\sigma$  for different surrogate models and query strategies. All the case studies begin with the same set of initial data points. The missing entries in the table correspond to case studies wherein  $R_g = 2.47\sigma$  is not achieved within the runtime of the AL cycle

Surrogate model query strategy	GPR		SVR		KRR	
	Kernel		Kernel		Kernel	
	RBF	Matérn	Linear	RBF	RBF	Laplacian
Pure exploitation	—	1552	1360	1744	1744	1264
Max. EI	—	1712	1296	1520	1744	1328
Max. PI	—	1232	—	—	1488	1457

iterations is far more pronounced compared to a random selection approach. Further, the pure exploration strategy shows poor convergence, with the  $R_g$  value being confined within a narrow range around  $2.80\sigma$ . In a few cases, it is even marginally outperformed by the random selection approach as shown in Fig. 3. Therefore, pure exploitation, Max-EI and Max-PI are able to circumvent local minima by intelligently sampling newer sequences that facilitate their convergence towards the global minima. For critically assessing the performance of different query strategies and surrogate models, the number of iterations required to identify a sequence with an average  $R_g$  of  $2.47\sigma$  is considered as a quantitative measure, and the number of MD simulations to achieve  $R_g = 2.47\sigma$  is tabulated in Table 1 for all the case studies. There are a few combinations of the surrogate model and the query strategy that did not yield  $R_g = 2.47\sigma$  within our predefined runtime of 75 epochs. They seem to cling to a suboptimal point above  $R_g = 2.47\sigma$  for a long period of time.

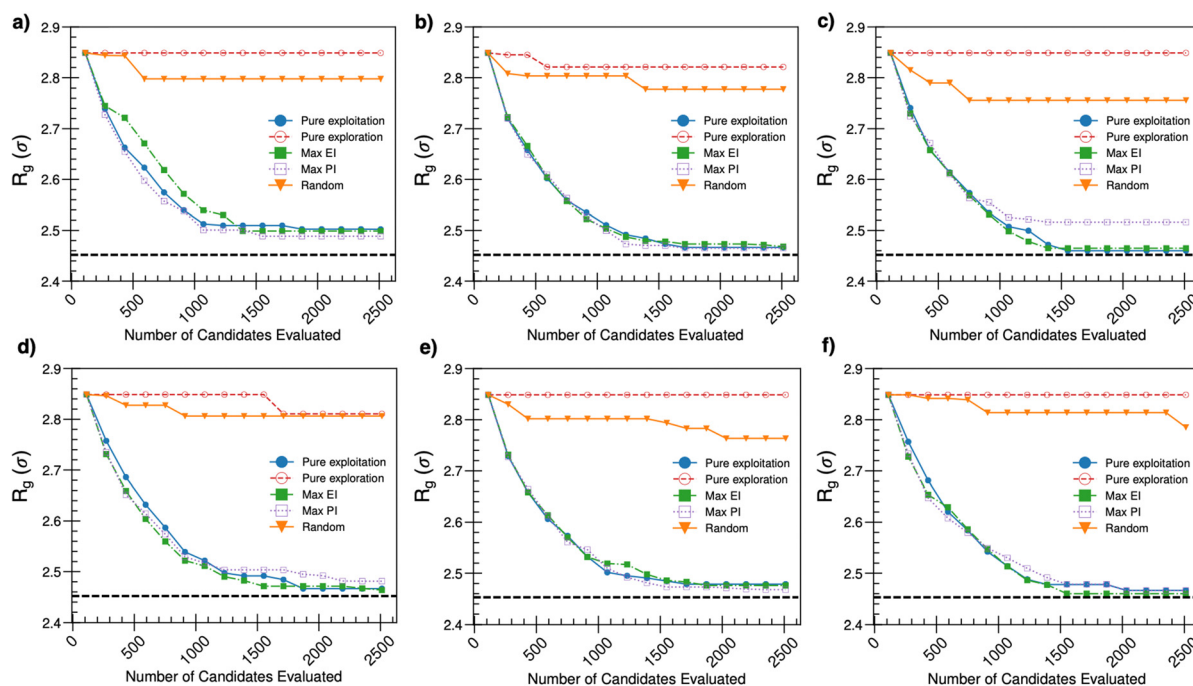


**Fig. 3** Active learning of radius of gyration of the copolymer using six surrogate models. The performance of active learning *via* GPR-RBF kernel, GPR-Matérn Kernel, SVR-Linear Kernel, SVR-RBF kernel, KRR-RBF kernel, and KRR-Laplacian kernel is shown in (a), (b), (c), (d), (e) and (f), respectively. For each of these six strategies, five different queries are used as mentioned in all the subplots.

Among all the case studies, we observe that the GPR (Matérn Kernel) with the Max-PI query strategy reaches the target by performing a lower number of MD simulations. Evidently, the quality of a solution and the required computational time for a design problem are very sensitive to the choices of the exact surrogate model and query strategy. The current MD simulation to compute the  $R_g$  of a sequence takes about 35 minutes in a single core of an Intel Xeon Gold 6248 high performance computing (HPC) node. We run  $32R_g$  calculations in parallel. A total of 720 hours of computing time is used to identify the optimal structure using GPR with the Max-PI query strategy.

### 3.2. Selection of query strategy

The impact of query strategies is analyzed for a representative case of the GPR model – Matérn kernel. Fig. 4 shows the spread of  $R_g$  values corresponding to the candidates that are sampled and appended to the training set at each iteration. The initial training set contains sequences whose  $R_g$  values span from  $2.84\sigma$  to  $5.03\sigma$ . This wide spread in the  $R_g$  value is reduced to a narrower breadth (spanning across  $2.7\sigma$  to  $3.0\sigma$ ) at the very first iteration of the active learning with the query strategies pure exploitation, Max-EI and Max-PI. This exemplifies the efficiency of these query strategies in selectively and rapidly eliminating the sampling of sequences with higher  $R_g$  values. The newer sequences that are sampled in subsequent iterations exhibit a fairly constant or mildly diminishing breadth of the spread in the  $R_g$  value, eventually resulting in a very narrow spread at the final iteration. For the pure exploration query strategy and the random selection, the  $R_g$  value spans across  $2.8\sigma$  to  $5.5\sigma$  for the entire range of iterations as shown in Fig. 4b and e, respectively. We note that the estimation of predictions and uncertainties (when the initial training set is fixed) by GPR does not have any dependency on the randomized bootstrap sampling, unlike SVR or KRR models. In SVR and KRR, for a particular query strategy, if the same initial training set is retained and the optimizer run multiple times, one might observe slightly different results every time owing to the differences in the bootstrap

sampling at every iteration. If one is extremely intent to eliminate the influences in optimizer performance arising out of variations in bootstrap sampling, GPR would be the best approach.

### 3.3. Stopping criteria for active learning

The stopping criterion, *i.e.*, the precise condition/circumstance at which the iterative process of active learning would be ceased, is an important aspect of a design algorithm. The general notion is to stop subsequent sampling when one is satisfied with the outcome of the target property or when one has run out of computational resources. In this work, we set the number of iterations to 75, and for most of them, the desired radius of gyration is obtained within 75 iterations. Owing to our theoretical understanding, we know that the minimum  $R_g$  would be found in a sequence that is predominantly populated by As, and hence the desired solution is not unknown *a priori*. However, determining such a stopping criterion is challenging for designing a sequence with a fixed A/B composition wherein the optimal solution can't be estimated analytically. Moreover, for problems involving longer sequences with an increased number of monomers wherein each computation of property (MD simulation) would be far more expensive, defining a stopping criterion becomes inevitable in order to save computational cost and time, and to avoid excessively scanning the sequence space. In such cases, one could consider a heuristic measure such as saturation in the marginal improvement of the optimizer over a considerable number of iterations. In Fig. 5, the incremental improvement in the performance of the optimizer is quantified for different query strategies by plotting the extent of the decrease in  $R_g$  as a function of the iteration number. For the query strategies pure exploitation, Max-EI, and Max-PI, the extent of decrease in  $R_g$  is high in the initial iterations, and becomes marginally small or fairly constant towards higher iterations (after 40–50 iterations, corresponding to roughly 1200–1600 MD simulations). For the pure exploration query strategy and the random selection approach, the extent of decrease in  $R_g$  becomes zero after a very few iterations, owing to

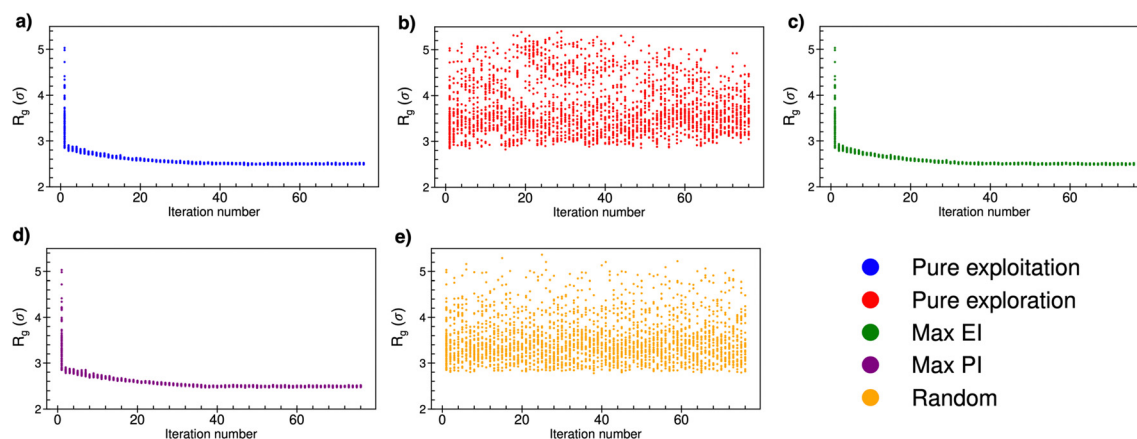


Fig. 4 Convergence of query strategies. The variation of  $R_g$  of the 32 candidates that are picked by a query strategy during an active learning cycle is shown as a function of the iteration number, for a specific surrogate model (Gaussian Process Regression with Matérn kernel) with query strategies pure exploitation, pure exploration, Max-EI, Max-PI, and random selection in (a), (b), (c), (d), and (e), respectively.

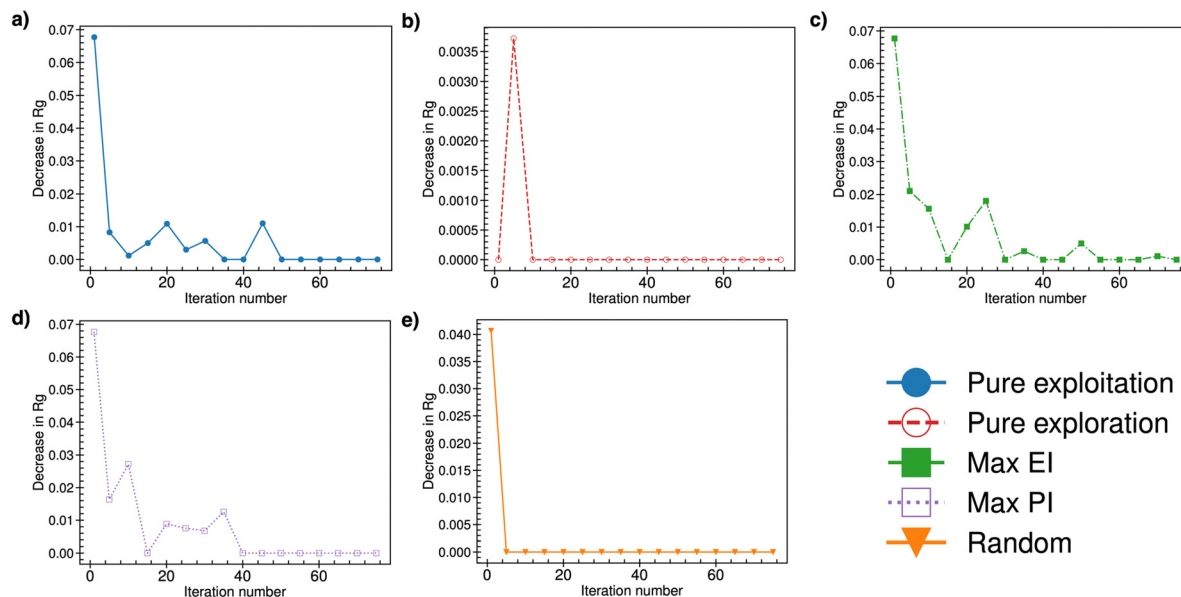


Fig. 5 Stopping criteria for different query strategies. The decrease in  $R_g$  is plotted as a function of the iteration number, for a specific surrogate model (GPR with Matérn kernel) with different query strategies.

the optimizer being stuck in a local optimum at a very early stage in the active learning cycle. Thus, it is recommended to consider the notion of incremental improvement cessation along with the larger perspective of convergence to the desired target property value, so as to avoid pre-mature or incorrect inferences. We note that a similar approach of quantifying the rate of improvement has been commonly used in the literature by means of an opportunity cost<sup>56</sup> concept which defines the modulus difference between the overall best value in the data set and the best-so-far. Along this line, Balachandran *et al.*<sup>57</sup> have formulated a stopping criterion by tracking the maximum expected improvement (Max-EI) at the end of each iteration. The recommendation is to not stop the iterative cycle immediately after Max-EI has reached a value of zero, but to run the iterative active learning loop for further iterations until Max-EI becomes consistently zero and does not further increase.

### 3.4. Assessment of surrogate models' quality during active learning

To assess the quality of surrogate models that are built progressively during an AL cycle, we test their performance for a data set of 32 new sequences. We compute the coefficient of determination ( $R^2$ ) with the true  $R_g$  values and predicted  $R_g$  values for 32 new candidates at the end of every iteration.  $R^2$  is computed as  $1 - \frac{SS_{\text{res}}}{SS_{\text{tot}}}$  wherein  $SS_{\text{res}}$  stands for the residual error and  $SS_{\text{tot}}$  stands for the total error. When  $\frac{SS_{\text{res}}}{SS_{\text{tot}}}$  is a small positive fraction, the model fitting is very good and this yields an  $R^2$  value close to 1. When  $SS_{\text{res}} > SS_{\text{tot}}$ , the model fitting is worse, and  $R^2$  ends up becoming negative. Fig. 6 compares the trends in  $R^2$  for a specific case of the GPR surrogate model (Matérn kernel) between pure exploitation and pure exploration query strategies. For the query strategy pure exploitation,  $R^2$  is

significantly negative across the 75 iterations indicating that the model is fairly inaccurate, as shown in Fig. 6a. The actual  $R_g$  and predicted  $R_g$  for the surrogate model that is built after the 75th iteration are shown in Fig. 6b. In spite of a bad quality surrogate model across the AL cycle, convergence towards optimal sequences is ensured. This indicates that the query strategy is progressively sampling candidates from outside the known range of properties and directing the search toward the extremum of the search space. Therefore, the active learning is quite forgiving of the quality of the surrogate model (even in the regime of large model error) as long as appropriate query strategies are employed to find optimal solutions. This observation is consistent with a previous design study for a different class of materials.<sup>56</sup> While the importance of model quality in the AL is an aspect that needs a lot of investigation and rigorous analysis, the current study tends to suggest that the iterative approach of active learning with the pure exploitation to sample newer candidates fairly guarantees high performance of the optimizer.

On the other hand, for pure exploration, which does not efficiently identify optimal sequences,  $R^2$  is positive and fairly close to 1 across the 75 iterations. This observation is expected, as the very intent of the pure exploration query strategy is to improve the model quality by continuously appending the training set by sampling data points which are predicted to have high uncertainty. The success of the surrogate models for the pure exploration strategy indicates that the new candidates are within or nearby region of the known range of property. Therefore, active learning within the pure exploration framework is not able to direct the search outside the known range of property, which is vital for identifying extremal candidates.

### 3.5. Selection of new candidates during active learning

At each iteration, a small search space is defined by enumerating the possible sequences that are sequentially proximate to

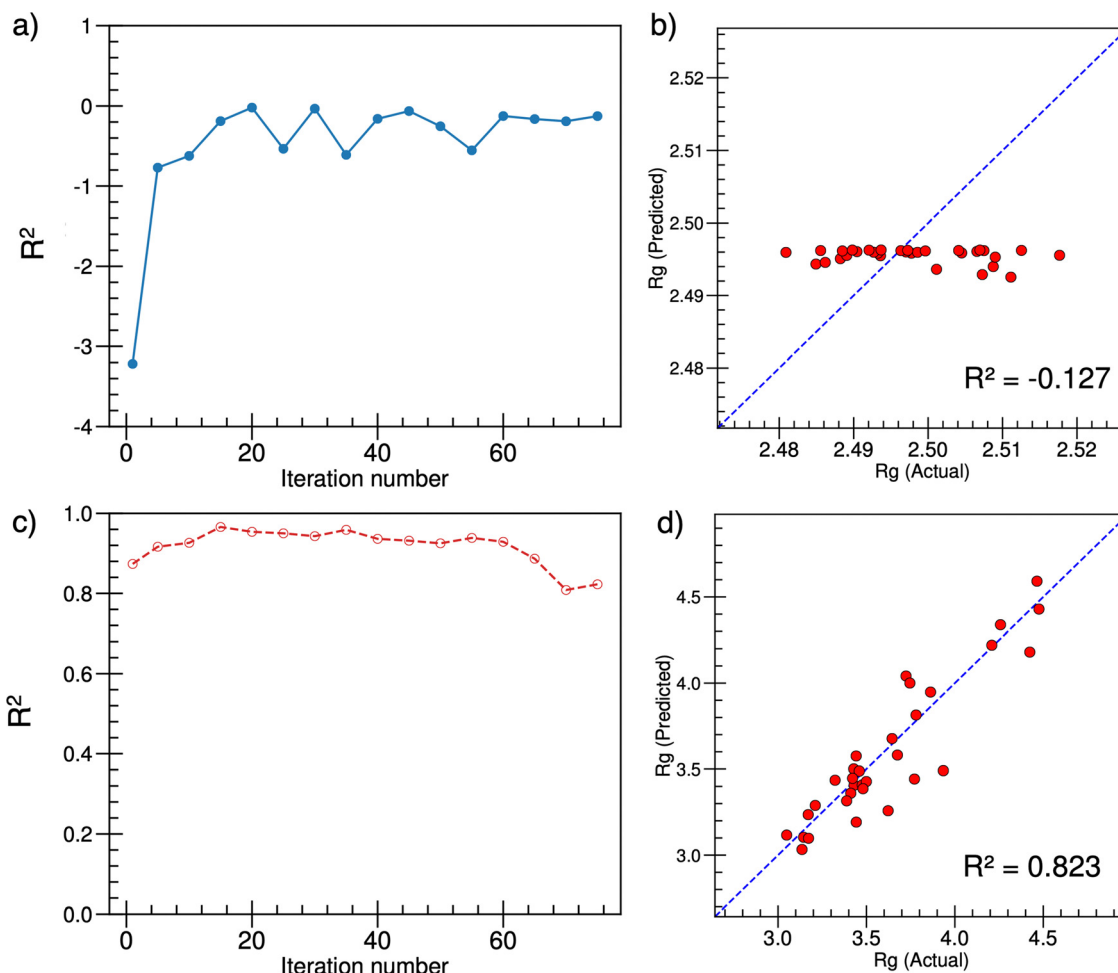


Fig. 6 The coefficient of determination ( $R^2$ ) of a GPR model with Matérn kernel is shown as a function of iteration number for active learning via (a) pure exploitation and (c) pure exploration. Predicted and actual  $R_g$  after the 75th iteration of the active learning cycle are compared in (b) and (d) for pure exploitation and pure exploration, respectively.

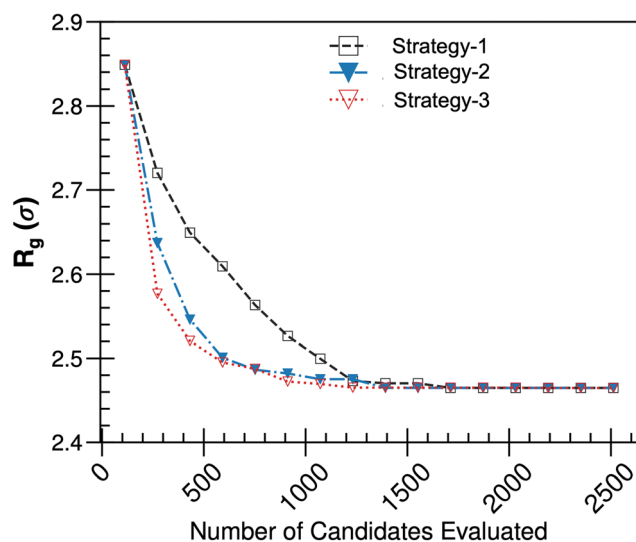


Fig. 7 Performance of an active learning algorithm for different strategies of selecting new candidates. The radius of gyration of the best candidate in each iteration is plotted as a function of the total number of candidates cumulatively screened via MD simulations during an active learning cycle.

the sequences in the training set accumulated until that particular iteration. For every copolymer sequence in the training set, the exhaustive list of copolymer sequences that differ in the monomeric entity at exactly one position (*i.e.*, one position of A replaced by B, or one position of B replaced by A) is considered to populate the search space. Here, we refer to this strategy as strategy-1. While such a candidate selection strategy indeed facilitates the convergence towards optimal candidates as shown in Fig. 3, the convergence can be accelerated by defining various selection methods. For example, we test two more strategies for candidate selection. In strategy-2, randomly selected four moieties change their types, and strategy-3 involves flipping the type of 10 moieties in the chain. We repeat the active learning cycle for these two new strategies and compare their performance with that of strategy-1 for a specific case of the GPR surrogate model with Matérn kernel and Max-PI query strategy. As shown in Fig. 7, the performance of strategy-2 and strategy-3 is very identical. However, the active learning process is significantly faster in strategy-2 and strategy-3 in comparison with strategy-1. Therefore, a binary flip of 4 monomers in a polymer of chain length  $N = 100$  appears to be more efficient for this sequence design problem. We note that



depending on the polymer size and complexity of the search space, one needs to identify the optimal number of binary flips that would lead to the faster convergence of the algorithm.

### 3.6. Scalability of active learning

We employ the best active learning strategy for designing a copolymer with varying chain length to understand the scalability of the design algorithm. For all the cases, we target to achieve the lowest  $R_g$  without any constraints in the composition of the chain using the GPR surrogate model with Matérn kernel and Max-PI query strategy. Fig. 8a shows the  $R_g$  values of the best candidate in a given iteration during an active learning cycle for a polymer of chain length  $N = 20, 50, 100$  and  $150$ . All of them converge to their optimal solutions within our simulation time. The minimum number of MD simulations to identify the optimal sequence for all the cases is shown in Fig. 8b. Evidentially, the number of MD simulations or physics-based property calculations that are required for the polymer design grows linearly with the chain length despite the search space growing exponentially. This suggests that the current algorithm scales well with the size and potentially accelerates the design of polymer sequences with target properties. We note that the actual computer time required for an  $R_g$  calculation is about 5, 11, 35 and 42 minutes for  $N = 20, 50, 100$  and  $150$ , respectively, in a single core of an Intel Xeon Gold 6248 HPC node.

### 3.7. Protein-like sequence design

A copolymer can form a compact protein-like core-shell structure in a dilute solution depending of its monomer sequence, and the extent of compactness of the aggregate is also dictated by its monomer to monomer sequence details.<sup>58,59</sup> Here, we aim to test the ability of the AL design algorithm for a complex design problem, *viz.*, identifying the sequence of a copolymer that produces the most compact core-shell structure. Based on the inferences drawn in the previous sections, we choose GPR (Matérn kernel) and Max-PI as the most efficient surrogate

model and query strategy, respectively, for identifying the compact core-shell structure of a copolymer of chain length  $N = 100$  and 1 : 1 composition ratio. Unlike the first problem, the optimal sequence for a compact core-shell structure is non-intuitive, non-periodic, and can't be estimated *a priori*. Similar to the previous case, here, our target property is the lowest radius of gyration, which can be considered as the measure of the most compact packing of the copolymer. Starting from a random sequence, we carry out an active learning cycle for designing the core-shell structure. We identify the lowest  $R_g$  of the copolymer by conducting 62 iterations of the active learning cycle. This corresponds to 1984 MD simulations. We calculate the density profiles of A-type and B-type moieties separately for the optimal structure as well as the initial structure in order to better understand the spatial arrangements of moieties. Two density profiles along with the equilibrium structures of the initial random sequence and the final optimal sequence are shown in Fig. 9. While the initial sequence (with  $R_g = 3.67\sigma$ ) has no clear distinct monomer-A dominated zones or monomer-B dominated zones, the optimal sequence (with  $R_g = 2.85\sigma$ ) demonstrates a distinct difference in the dominance of monomer units A and B at different radial distances. The conformational structure of the optimal sequence has a dense core dominated by monomer A with the periphery dominated by monomer B, resulting in a spherical globule-like structure. Such a distinct core-shell structure formed by different chemical species quite resembles three-dimensional protein structures, which have a packing of hydrophobic moieties in the core and polar groups on the periphery. Thus, the AL framework efficiently scans the astronomically large search space of a copolymer and identifies its sequence that leads to a closed packing of its monomers in an implicit dilute solution condition by performing over 2000 MD calculations, which is about 1200 hours of computing time in a single core of an Intel Xeon Gold 6248 HPC node. Previously, Khokhlov and Khalatur<sup>60</sup> introduced a "coloring" scheme to design protein-like sequences in a computer simulation, wherein the surface particles of a

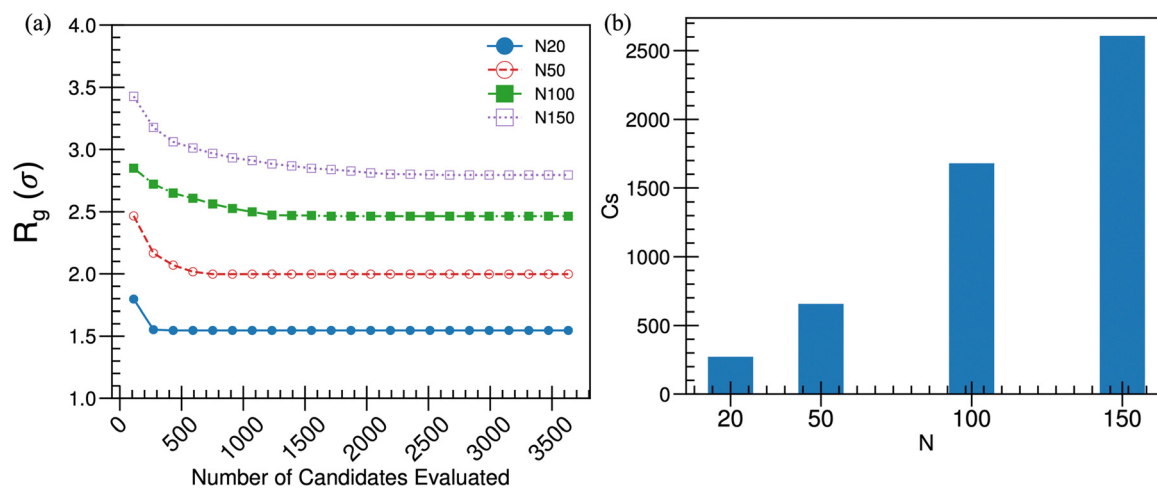


Fig. 8 Scaling analysis. (a) The lowest radius of gyration during an active learning cycle is plotted as a function of number of MD simulations that are completed until a particular iteration of the active learning cycle for four case studies. (b) Minimum number of MD simulations to achieve an optimal candidate in a design cycle is shown for all four case studies.

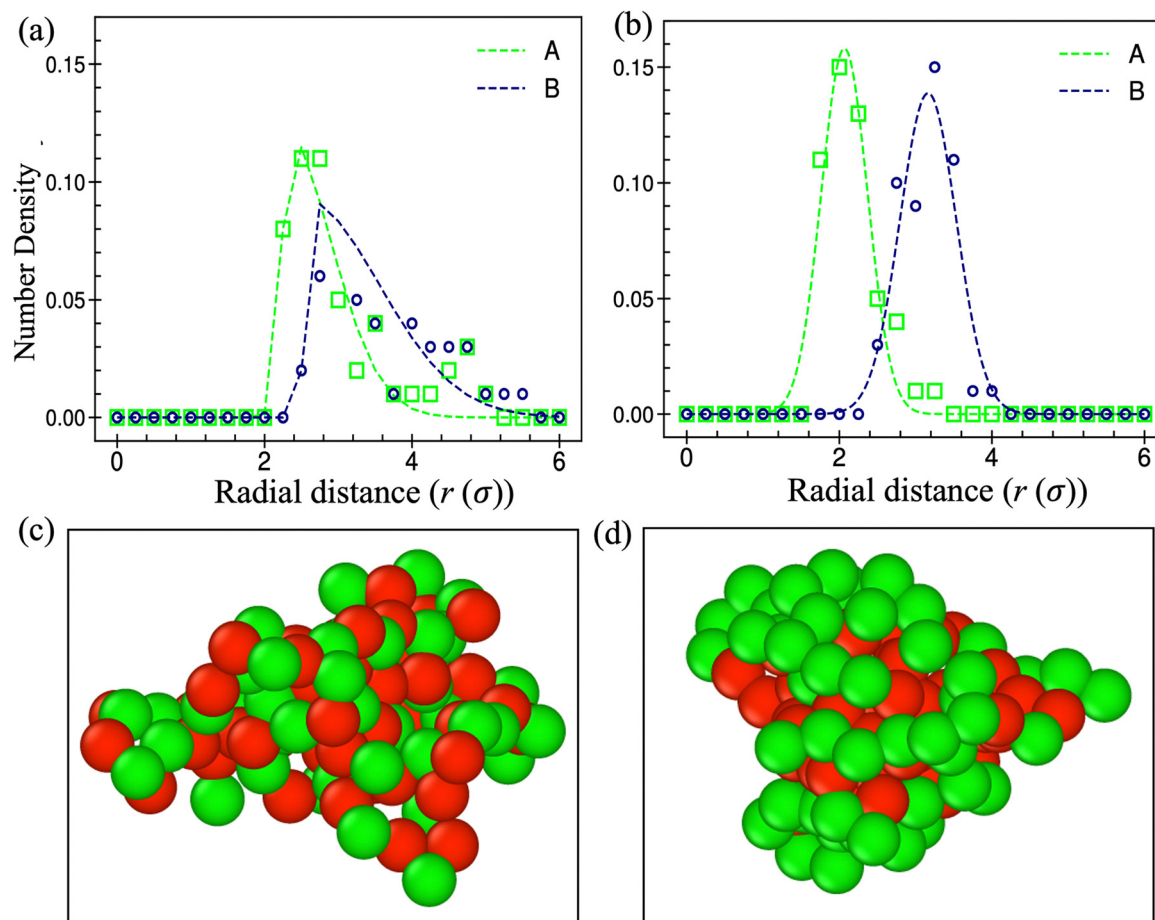


Fig. 9 Protein-like sequence design. Density profile of A- and B-type moieties from the centroid of the globule for a randomly chosen sequence and an AL-identified sequence for a copolymer of chain length  $N = 100$  with an equal proportion of A- and B-type moieties is shown in (a) and (b), respectively. The respective MD snapshots are shown in (c) and (d).

collapsed homopolymer are assigned with hydrophilic interaction while the particles in the core are assigned with hydrophobic interaction. Although this protocol will produce a core-shell structure, the designed sequence may not capture the reversible denaturation phenomenon in a manner that is reminiscent of proteins. To address this issue, Sharma *et al.* have developed a coarse-grained protein model in a water-like solvent using Monte Carlo simulations.<sup>61</sup> The current case study is motivated by these previous works. However, the current MD simulation-based active learning method treats the solvent implicitly, and it evolves from a random copolymer. Thus our method is computationally faster and can identify sequences that can exhibit reversible denaturation. We expect that the current AL-identified protein-like sequences can be used to study the thermodynamics of folding, denaturation, misfolding, multi-molecular aggregation and adsorption in a manner that is reminiscent of real proteins in a computationally efficient way.

## 4. Conclusions

Active learning has emerged as an attractive tool for materials design. The performance of an active learning framework

depends on many factors such as the surrogate model, initial data set, query strategy, uncertainty quantification, selection of search space, and stopping criteria. The implications of these choices are profound for problems with complex search space and high computational costs. Here, we survey some of these critical aspects of active learning for a polymer design problem. As a proof of concept, we choose the single-molecule radius of gyration of a copolymer as a target property to establish the most efficient active learning strategy. We consider a model copolymer with two chemically dissimilar moieties and conduct a CGMD simulation to compute its radius of gyration in an implicit solvent condition. This CGMD simulation is integrated within an active learning framework to identify a copolymer sequence with the lowest radius of gyration. We first identify optimal strategies and parameters by targeting an analytically known solution. The GPR (Matérn kernel) and Max-PI are found to be the most efficient surrogate model and query strategy, respectively, for the sequence design problem. Moreover, we test the efficacy of the best active learning strategy to identify a copolymer sequence that produces a compact core-shell structure, similar to a folded protein. The present work uses the active learning method for sequence optimization, and it can

be further extended to optimize the composition ratio, copolymer chain length, and cross-interaction between the moieties to achieve a target shape and size of the aggregate. We also use a very generic phenomenological model of a copolymer in an implicit solvent condition to establish the active learning framework. However, this method can be directly used for sequence optimization of an atomistic model of a copolymer with explicit solvents and multimolecular systems with increasingly complex design tasks. The current study presents a thorough analysis of commonly used active learning strategies for polymer sequence design problems and will be useful for sequence engineering, which is gaining popularity and potency for materials design.

## Code and data availability

Example scripts demonstrating the construct of the active learning method are available at [https://github.com/rpspran/Polymer\\_Sequence\\_Design](https://github.com/rpspran/Polymer_Sequence_Design). Additional data related to this paper may be requested from the authors.

## Conflicts of interest

There are no conflicts to declare.

## Acknowledgements

The work is made possible by financial support from SERB, DST, Govt of India through a start-up research grant (SRG/2020/001045) and National Supercomputing Mission's research grant (DST/NSM/R&D\_HPC\_Applications/2021/40). This research used resources of the Argonne Leadership Computing Facility, which is a DOE Office of Science User Facility supported under Contract DE-AC02-06CH11357. We also used the computational facility of the Center for Nanoscience Materials. Use of the Center for Nanoscale Materials, an Office of Science user facility, was supported by the U.S. Department of Energy, Office of Science, Office of Basic Energy Sciences, under Contract No. DE-AC02-06CH11357. We acknowledge the use of the computing resources at HPCE, IIT Madras.

## References

- 1 M. Porel and C. A. Alabi, Sequence-Defined Polymers via Orthogonal Allyl Acrylamide Building Blocks, *J. Am. Chem. Soc.*, 2014, **136**(38), 13162–13165, DOI: [10.1021/ja507262t](#).
- 2 H. J. Olivos, P. G. Alluri, M. M. Reddy, D. Salony and T. Kodadek, Microwave-Assisted Solid-Phase Synthesis of Peptoids, *Org. Lett.*, 2002, **4**(23), 4057–4059, DOI: [10.1021/ol0267578](#).
- 3 T. T. Trinh, L. Oswald, D. Chan-Seng and J.-F. Lutz, Synthesis of Molecularly Encoded Oligomers Using a Chemoselective “AB + CD” Iterative Approach, *Macromol. Rapid Commun.*, 2014, **35**(2), 141–145, DOI: [10.1002/marc.201300774](#).
- 4 M. Porel, D. N. Thornlow, N. N. Phan and C. A. Alabi, Sequence-Defined Bioactive Macrocycles via an Acid-Catalysed Cascade Reaction, *Nat. Chem.*, 2016, **8**(6), 590–596, DOI: [10.1038/nchem.2508](#).
- 5 R. Dong, R. Liu, P. R. J. Gaffney, M. Schaepertoens, P. Marchetti, C. M. Williams, R. Chen and A. G. Livingston, Sequence-Defined Multifunctional Polyethers via Liquid-Phase Synthesis with Molecular Sieving, *Nat. Chem.*, 2019, **11**(2), 136–145, DOI: [10.1038/s41557-018-0169-6](#).
- 6 C. F. Buitrago, D. S. Bolintineanu, M. E. Seitz, K. L. Opper, K. B. Wagener, M. J. Stevens, A. L. Frischknecht and K. I. Winey, Direct Comparisons of X-Ray Scattering and Atomistic Molecular Dynamics Simulations for Precise Acid Copolymers and Ionomers, *Macromolecules*, 2015, **48**(4), 1210–1220, DOI: [10.1021/ma5022117](#).
- 7 T. K. Patra, T. D. Loeffler and S. K. R. S. Sankaranarayanan, Accelerating Copolymer Inverse Design Using Monte Carlo Tree Search, *Nanoscale*, 2020, **12**(46), 23653–23662, DOI: [10.1039/D0NR06091G](#).
- 8 S. L. Perry and C. E. Sing, 100th Anniversary of Macromolecular Science Viewpoint: Opportunities in the Physics of Sequence-Defined Polymers, *ACS Macro Lett.*, 2020, **9**(2), 216–225, DOI: [10.1021/acsmacrolett.0c00002](#).
- 9 A. Al Ouahabi, M. Kotera, L. Charles and J.-F. Lutz, Synthesis of Monodisperse Sequence-Coded Polymers with Chain Lengths above DP100, *ACS Macro Lett.*, 2015, **4**(10), 1077–1080, DOI: [10.1021/acsmacrolett.5b00606](#).
- 10 T. K. Lytle, L.-W. Chang, N. Markiewicz, S. L. Perry and C. E. Sing, Designing Electrostatic Interactions via Polyelectrolyte Monomer Sequence, *ACS Cent. Sci.*, 2019, **5**(4), 709–718, DOI: [10.1021/acscentsci.9b00087](#).
- 11 C. E. Sing, Micro- to Macro-Phase Separation Transition in Sequence-Defined Coacervates, *J. Chem. Phys.*, 2020, **152**(2), 024902, DOI: [10.1063/1.5140756](#).
- 12 L.-W. Chang, T. K. Lytle, M. Radhakrishna, J. J. Madinya, J. Vélez, C. E. Sing and S. L. Perry, Sequence and Entropy-Based Control of Complex Coacervates, *Nat. Commun.*, 2017, **8**(1), 1273, DOI: [10.1038/s41467-017-01249-1](#).
- 13 J. J. Madinya, L.-W. Chang, S. L. Perry and C. E. Sing, Sequence-Dependent Self-Coacervation in High Charge-Density Polyampholytes, *Mol. Syst. Des. Eng.*, 2020, **5**(3), 632–644, DOI: [10.1039/C9ME00074G](#).
- 14 M. E. Gindy, R. K. Prud'homme and A. Z. Panagiotopoulos, Phase Behavior and Structure Formation in Linear Multiblock Copolymer Solutions by Monte Carlo Simulation, *J. Chem. Phys.*, 2008, **128**(16), 164906, DOI: [10.1063/1.2905231](#).
- 15 Y. Chushak and A. Travesset, Coarse-Grained Molecular-Dynamics Simulations of the Self-Assembly of Pentablock Copolymers into Micelles, *J. Chem. Phys.*, 2005, **123**(23), 234905, DOI: [10.1063/1.2137714](#).
- 16 W. F. Reinhart and A. Statt, Opportunities and Challenges for Inverse Design of Nanostructures with Sequence Defined Macromolecules, *Acc. Mater. Res.*, 2021, **2**(9), 697–700, DOI: [10.1021/accountsmr.1c00089](#).
- 17 V. Meenakshisundaram, J.-H. Hung, T. K. Patra and D. S. Simmons, Designing Sequence-Specific Copolymer Compatibilizers Using a Molecular-Dynamics-Simulation-Based Genetic Algorithm, *Macromolecules*, 2017, **50**(3), 1155–1166, DOI: [10.1021/acs.macromol.6b01747](#).

- 18 A. Statt, H. Casademunt, C. P. Brangwynne and A. Z. Panagiotopoulos, Model for Disordered Proteins with Strongly Sequence-Dependent Liquid Phase Behavior, *J. Chem. Phys.*, 2020, **152**(7), 075101, DOI: [10.1063/1.5141095](#).
- 19 A. Statt, D. C. Kleeblatt and W. F. Reinhart, Unsupervised Learning of Sequence-Specific Aggregation Behavior for a Model Copolymer, *Soft Matter*, 2021, **17**(33), 7697–7707, DOI: [10.1039/D1SM01012C](#).
- 20 V. Meenakshisundaram, J.-H. Hung, T. K. Patra and D. S. Simmons, Designing Sequence-Specific Copolymer Compatibilizers Using a Molecular-Dynamics-Simulation-Based Genetic Algorithm, *Macromolecules*, 2017, **50**(3), 1155–1166, DOI: [10.1021/acs.macromol.6b01747](#).
- 21 W. F. Drayer and D. S. Simmons, Sequence Effects on the Glass Transition of a Model Copolymer System, *Macromolecules*, 2022, **55**(14), 5926–5937, DOI: [10.1021/acs.macromol.2c00664](#).
- 22 D. K. Tulsi and D. S. Simmons, Hierarchical Shape-Specified Model Polymer Nanoparticles via Copolymer Sequence Control, *Macromolecules*, 2022, **55**(6), 1957–1969, DOI: [10.1021/acs.macromol.1c02215](#).
- 23 J.-F. Lutz, M. Ouchi, D. R. Liu and M. Sawamoto, Sequence-Controlled Polymers, *Science*, 2013, **341**(6146), 1238149, DOI: [10.1126/science.1238149](#).
- 24 L. Chen, G. Pilania, R. Batra, T. D. Huan, C. Kim, C. Kuenneth and R. Ramprasad, Polymer Informatics: Current Status and Critical Next Steps, *Materials Science and Engineering: R: Reports*, 2021, **144**, 100595, DOI: [10.1016/j.mser.2020.100595](#).
- 25 A. J. Gormley and M. A. Webb, Machine Learning in Combinatorial Polymer Chemistry, *Nat Rev Mater*, 2021, **6**(8), 642–644, DOI: [10.1038/s41578-021-00282-3](#).
- 26 M. A. Webb, N. E. Jackson, P. S. Gil and J. J. de Pablo, Targeted Sequence Design within the Coarse-Grained Polymer Genome, *Sci. Adv.*, 2020, **6**(43), eabc6216, DOI: [10.1126/sciadv.abc6216](#).
- 27 T. K. Patra, Data-Driven Methods for Accelerating Polymer Design, *ACS Polym. Au*, 2022, **2**(1), 8–26, DOI: [10.1021/acspolymersau.1c00035](#).
- 28 S. Dasetty, I. Coropceanu, J. Portner, J. Li, J. J. Pablo, D. de; Talapin and A. L. Ferguson, Active Learning of Polarizable Nanoparticle Phase Diagrams for the Guided Design of Triggerable Self-Assembling Superlattices, *Mol. Syst. Des. Eng.*, 2022, **7**(4), 350–363, DOI: [10.1039/D1ME00187F](#).
- 29 B. Mohr, K. Shmilovich, I. S. Kleinwächter, D. Schneider, A. L. Ferguson and T. Bereau, Data-Driven Discovery of Cardiolipin-Selective Small Molecules by Computational Active Learning, *Chem. Sci.*, 2022, **13**(16), 4498–4511, DOI: [10.1039/D2SC00116K](#).
- 30 C. Dai and S. C. Glotzer, Efficient Phase Diagram Sampling by Active Learning, *J. Phys. Chem. B*, 2020, **124**(7), 1275–1284, DOI: [10.1021/acs.jpcc.9b09202](#).
- 31 G. Agarwal, H. A. Doan, L. A. Robertson, L. Zhang and R. S. Assary, Discovery of Energy Storage Molecular Materials Using Quantum Chemistry-Guided Multiobjective Bayesian Optimization, *Chem. Mater.*, 2021, **33**(20), 8133–8144, DOI: [10.1021/acs.chemmater.1c02040](#).
- 32 T. Lookman, P. V. Balachandran, D. Xue, J. Hogden and J. Theiler, Statistical Inference and Adaptive Design for Materials Discovery, *Curr. Opin. Solid State Mater. Sci.*, 2017, **21**(3), 121–128, DOI: [10.1016/j.cossms.2016.10.002](#).
- 33 D. Xue, Y. Tian, R. Yuan and T. Lookman, Bayesian Global Optimization Applied to the Design of Shape-Memory Alloys, in *Uncertainty Quantification in Multiscale Materials Modeling*, Elsevier, 2020, pp. 519–537, DOI: [10.1016/B978-0-08-102941-1.00016-X](#).
- 34 A. Mannodi-Kanakkithodi, A. Chandrasekaran, C. Kim, T. D. Huan, G. Pilania, V. Botu and R. Ramprasad, Scoping the Polymer Genome: A Roadmap for Rational Polymer Dielectrics Design and Beyond, *Mater. Today*, 2018, **21**(7), 785–796, DOI: [10.1016/j.mattod.2017.11.021](#).
- 35 P. V. Balachandran, D. Xue, J. Theiler, J. Hogden and T. Lookman, Adaptive Strategies for Materials Design Using Uncertainties, *Sci. Rep.*, 2016, **6**(1), 19660, DOI: [10.1038/srep19660](#).
- 36 D. Xue, P. V. Balachandran, J. Hogden, J. Theiler, D. Xue and T. Lookman, Accelerated Search for Materials with Targeted Properties by Adaptive Design, *Nat. Commun.*, 2016, **7**(1), 11241, DOI: [10.1038/ncomms11241](#).
- 37 A. Mannodi-Kanakkithodi, G. Pilania, T. D. Huan, T. Lookman and R. Ramprasad, Machine Learning Strategy for Accelerated Design of Polymer Dielectrics, *Sci. Rep.*, 2016, **6**(1), 20952, DOI: [10.1038/srep20952](#).
- 38 D. Bhattacharya, D. C. Kleeblatt, A. Statt and W. F. Reinhart, Predicting Aggregate Morphology of Sequence-Defined Macromolecules with Recurrent Neural Networks, *Soft Matter*, 2022, **18**(27), 5037–5051, DOI: [10.1039/D2SM000452F](#).
- 39 J. Shi, M. J. Quevillon, P. H. A. Valença and J. K. Whitmer, Predicting Adhesive Free Energies of Polymer–Surface Interactions with Machine Learning, *ACS Appl. Mater. Interfaces*, 2022, **14**(32), 37161–37169, DOI: [10.1021/acsami.2c08891](#).
- 40 R. A. Patel, C. H. Borca and M. A. Webb, Featurization Strategies for Polymer Sequence or Composition Design by Machine Learning, *Mol. Syst. Des. Eng.*, 2022, **7**(6), 661–676, DOI: [10.1039/D1ME00160D](#).
- 41 K. M. Jablonka, G. M. Jothiappan, S. Wang, B. Smit and B. Yoo, Bias Free Multiobjective Active Learning for Materials Design and Discovery, *Nat. Commun.*, 2021, **12**(1), 2312, DOI: [10.1038/s41467-021-22437-0](#).
- 42 D. E. Dunstan, The Viscosity-Radius Relationship for Concentrated Polymer Solutions, *Sci. Rep.*, 2019, **9**(1), 543, DOI: [10.1038/s41598-018-36596-6](#).
- 43 T. Zhou, Z. Wu, H. K. Chilukoti and F. Müller-Plathe, Sequence-Engineering Polyethylene–Polypropylene Copolymers with High Thermal Conductivity Using a Molecular-Dynamics-Based Genetic Algorithm, *J. Chem. Theory Comput.*, 2021, **17**(6), 3772–3782, DOI: [10.1021/acs.jctc.1c00134](#).
- 44 K. Kremer and G. S. Grest, Dynamics of Entangled Linear Polymer Melts: A Molecular-dynamics Simulation, *J. Chem. Phys.*, 1990, **92**(8), 5057–5086, DOI: [10.1063/1.458541](#).
- 45 W. Wang, P. Zhao, X. Yang and Z.-Y. Lu, Coil-to-Globule Transitions of Homopolymers and Multiblock Copolymers, *J. Chem. Phys.*, 2014, **141**(24), 244907, DOI: [10.1063/1.4904888](#).



- 46 A. A. Bale, S. M. B. Gautham and T. K. Patra, Sequence-Defined Pareto Frontier of a Copolymer Structure, *J. Polym. Sci.*, 2022, **60**(14), 2100–2113, DOI: [10.1002/pol.20220088](https://doi.org/10.1002/pol.20220088).
- 47 S. Plimpton, Fast Parallel Algorithms for Short-Range Molecular Dynamics, *J. Comput. Phys.*, 1995, **117**(1), 1–19, DOI: [10.1006/jcph.1995.1039](https://doi.org/10.1006/jcph.1995.1039).
- 48 LAMMPS Molecular Dynamics Simulator. <https://www.lammps.org/>(accessed 2021-09-13).
- 49 E. Brochu, V. M. Cora and N. de Freitas, *A Tutorial on Bayesian Optimization of Expensive Cost Functions, with Application to Active User Modeling and Hierarchical Reinforcement Learning*, *arXiv*, 2010, 1012.2599v1, DOI: [10.48550/arXiv.1012.2599](https://doi.org/10.48550/arXiv.1012.2599).
- 50 D. Xue, Y. Tian, R. Yuan and T. Lookman, Bayesian Global Optimization Applied to the Design of Shape-Memory Alloys, in *Uncertainty Quantification in Multiscale Materials Modeling*, Elsevier, 2020, pp. 519–537, DOI: [10.1016/B978-0-08-102941-1.00016-X](https://doi.org/10.1016/B978-0-08-102941-1.00016-X).
- 51 T. Lookman, P. V. Balachandran, D. Xue and R. Yuan, Active Learning in Materials Science with Emphasis on Adaptive Sampling Using Uncertainties for Targeted Design, *npj Comput. Mater.*, 2019, **5**(1), 21, DOI: [10.1038/s41524-019-0153-8](https://doi.org/10.1038/s41524-019-0153-8).
- 52 Z. Chen and B. Wang, How Priors of Initial Hyperparameters Affect Gaussian Process Regression Models, *Neurocomputing*, 2018, **275**, 1702–1710, DOI: [10.1016/j.neucom.2017.10.028](https://doi.org/10.1016/j.neucom.2017.10.028).
- 53 A. Stuke, P. Rinke and M. Todorović, Efficient Hyperparameter Tuning for Kernel Ridge Regression with Bayesian Optimization, *Mach. Learn.: Sci. Technol.*, 2021, **2**(3), 035022, DOI: [10.1088/2632-2153/abec59](https://doi.org/10.1088/2632-2153/abec59).
- 54 F. Pedregosa, G. Varoquaux, A. Gramfort, V. Michel, B. Thirion, O. Grisel, M. Blondel, P. Prettenhofer, R. Weiss, V. Dubourg, J. Vanderplas, A. Passos, D. Cournapeau, M. Brucher, M. Perrot and É. Duchesnay, Scikit-Learn: Machine Learning in Python, *J. Mach. Learn. Res.*, 2011, **12**(85), 2825–2830.
- 55 *scikit-learn: machine learning in Python—scikit-learn 0.24.2 documentation*. <https://scikit-learn.org/stable/index.html> (accessed 2021-09-15).
- 56 P. V. Balachandran, D. Xue, J. Theiler, J. Hogden and T. Lookman, Adaptive Strategies for Materials Design Using Uncertainties, *Sci. Rep.*, 2016, **6**(1), 19660, DOI: [10.1038/srep19660](https://doi.org/10.1038/srep19660).
- 57 P. V. Balachandran, D. Xue, J. Theiler, J. Hogden, J. E. Gubernatis and T. Lookman, Importance of Feature Selection in Machine Learning and Adaptive Design for Materials, in *Materials Discovery and Design*, ed. T. Lookman, S. Eidenbenz, F. Alexander and C. Barnes, Springer International Publishing, Cham, 2018, vol. 280, pp. 59–79, DOI: [10.1007/978-3-319-99465-9\\_3](https://doi.org/10.1007/978-3-319-99465-9_3).
- 58 A. K. Dasmahapatra, G. Kumaraswamy and H. Nanavati, Collapse Transition in Random Copolymer Solutions, *Macromolecules*, 2006, **39**(26), 9621–9629, DOI: [10.1021/ma061017q](https://doi.org/10.1021/ma061017q).
- 59 A. K. Dasmahapatra, H. Nanavati and G. Kumaraswamy, Pathway to Copolymer Collapse in Dilute Solution: Uniform versus Random Distribution of Comonomers, *J. Chem. Phys.*, 2007, **127**(23), 234901, DOI: [10.1063/1.2802296](https://doi.org/10.1063/1.2802296).
- 60 A. R. Khokhlov and P. G. Khalatur, Protein-like Copolymers: Computer Simulation, *Phys. A*, 1998, **249**(1), 253–261, DOI: [10.1016/S0378-4371\(97\)00473-1](https://doi.org/10.1016/S0378-4371(97)00473-1).
- 61 S. Sharma, S. K. Kumar, S. V. Buldyrev, P. G. Debenedetti, P. J. Rossky and H. E. Stanley, A Coarse-Grained Protein Model in a Water-like Solvent, *Sci. Rep.*, 2013, **3**(1), 1841, DOI: [10.1038/srep01841](https://doi.org/10.1038/srep01841).